

Nature of the native-defect ESR and hydrogen-dangling-bond centers in thin diamond films

H. Jia and J. Shinar

Ames Laboratory and Physics and Astronomy Department, Iowa State University, Ames, Iowa 50011

D. P. Lang and M. Pruski

Ames Laboratory and Chemistry Department, Iowa State University, Ames, Iowa 50011

(Received 24 August 1993)

The X-band ESR of thin diamond films deposited from a mixture of 99.5% H₂ and 0.5% CH₄ is compared to those of films similarly prepared from D₂-CD₄ and H₂-¹³CH₄ mixtures. The main line and the satellites at ±7.2 G are unaffected by annealing at $T \leq 1100^\circ\text{C}$, but their intensity is reduced upon annealing at $\sim 1500^\circ\text{C}$. Since the satellites are absent from the deuterated films, they are attributed to newly identified dangling-bond H centers, possibly on internal surfaces, but more plausibly embedded in the bulk. This is consistent with the ¹³C relaxation rate, which indicates a uniform distribution of paramagnetic centers.

Extensive studies on thin diamond films have been reported since the discovery that they could be deposited on hot substrates by thermally assisted chemical vapor deposition (CVD) of CH₄ heavily diluted by H₂.^{1,2} The widespread activity in this area is largely motivated by their technological potential as excellent heat-conducting substrates for microelectronic circuitry,³ hard transparent coatings, and as the emissive layers of violet-blue light-emitting diodes.³ Relatively modest efforts, however, have been directed towards establishing a detailed picture of the structural and electronic properties of these films in general and their native defects in particular.^{1,2,4-6} This paper focuses on the nature of the ESR that is invariably observed in these films, and is thus evidently due to a native defect. This ESR includes a central line that usually appears to be the sum of narrow and broad Lorentzians, both at $g = 2.0025 \pm 0.0005$, of derivative peak-to-peak widths $\Delta H_{ppn} = 1.4 \pm 0.2$ and $3.0 \leq \Delta H_{ppb} \leq 6.1$ G.⁴⁻⁷ In many cases, but not all, two partially resolved satellites are observed at $\Delta g \approx \pm 3.6 \times 10^{-3} - \pm 4.3 \times 10^{-3}$ ($\Delta H \approx \pm 6.0 - \pm 7.5$ G at the X-band frequency of 9.33 GHz).⁴⁻⁷ We show below that the main line and the satellites at ±7.2 G are unaffected by annealing at $T \leq 1100^\circ\text{C}$, but their intensity is reduced upon annealing at $\sim 1500^\circ\text{C}$. Yet the satellites are strikingly absent from the ESR of films deposited from a mixture of 99.5% D₂ and 0.5% CD₄ or 99.5% D₂ and 0.5% CH₄. They are thus attributed to intrinsic spin- $\frac{1}{2}$ defects hyperfine-coupled to adjacent ¹H. To the best of our knowledge, these centers have not been previously detected in either natural,⁸ synthetic,⁹ or CVD films of diamond. Most of the hydrogen in as-deposited films is believed to be confined to the diamond crystallite surfaces,^{6,10-12} and NMR studies show that it evolves from the films after annealing for 2 h at $\sim 850^\circ\text{C}$.¹³ These newly identified dangling-bond-H centers are therefore suspected to be bulk defects. The ¹³C spin-lattice relaxation time T_1 in these films, as well as in fully ¹³C-enriched films, which indicates a homogeneous distribution of paramagnetic relaxation centers, is consistent with this assignment. The detailed structure of the dangling bonds which yield the central ESR line is not clear, but some

possibilities are discussed.

Thin diamond films were grown by flowing a 99.5% H₂-0.5% CH₄ or a similar D₂-CD₄ mixture at a pressure of ~ 50 torr and a flow rate of ~ 200 sccm through a tungsten filament heated to $\sim 2000^\circ\text{C}$ and onto an Si wafer substrate heated to 850°C . The growth rate of the films was ~ 0.5 $\mu\text{m}/\text{h}$. Following the deposition, the Si substrate was removed by dissolving it in HF, to yield free-standing films. X-ray-diffraction spectra yielded sharp diamond diffraction peaks only.

The films were oven annealed in either open quartz tubes in an Ar flow, or in sealed evacuated quartz tubes, or by an oxyacetylene torch in an open quartz tube in an Ar flow.

The ¹H and ¹³C NMR was measured at 100.06 and 25.16 MHz, respectively, using a homebuilt spectrometer. The ¹H spin count was performed using single pulse excitation, averaging over 1000 free-induction decay responses, and comparing to water. The ¹³C T_1 was measured under high resolution, by magic angle spinning at 4.5 kHz, with the progressive saturation method. Additional details are provided elsewhere.¹⁴ The ¹³C NMR of naturally (1.1%) abundant as well as of 99% ¹³C-enriched films indicated that no more than 0.5% of the carbon atoms are in a nondiamond configuration.¹⁴ No nitrogen ESR, identifiable by the ¹⁴N hyperfine-split components at $\pm 25 - \pm 330$ G from the main line,⁴ could be detected by the Bruker DSR 200 ESR spectrometer. Scanning electron microscopy (SEM) showed that the crystallites at the top surface of the film are several micrometers across. The ¹H NMR spin count, however, suggested that if the hydrogen was confined to the crystallite surfaces and essentially covered them, then the average crystallite should be less than ~ 0.5 μm across.¹⁴ This apparent discrepancy may be due to the observation that the crystallite size increases during film growth^{10,11,15} and the smaller crystallites near the substrate cannot be seen in SEM images. These smaller crystallites could account for the larger amount of hydrogen detected by NMR. This issue is discussed further below.

Typical X-band derivative ESR spectra of samples *A* and *B* deposited from H₂-CH₄, the former grown over 30

h, the latter over 146 h, are shown as the solid lines in Figs. 1(a) and 1(b), respectively. The total integrated intensities yield spin densities of 3.1×10^{16} and 2.7×10^{17} spins/g, or 0.6 and 5.4 ppm, respectively. The observation that the spin density of the thicker film *B* is greater than that of the thinner one *A* is interesting but not understood at present. Following Redwing, Root, and Banholzer,⁶ the spectra were fit to the sum of four Lorentzians (shown as the dotted lines in Fig. 1), of *g* values, amplitudes, and linewidths summarized in Table I. The central narrow and broad Lorentzians, invariably observed in all films, have been attributed to exchange-narrowed clusters and isolated carbon dangling bonds at spinless ^{12}C nuclei, respectively.⁶ However, the detailed structure of neither of these centers was addressed and we are not aware of model calculations that would hypothesize their structure. The satellites were suggested to result from hyperfine coupling of carbon dangling bonds with central or adjacent ^{13}C nuclei, or with neighboring ^1H .⁶ The former interpretation, however, is problematic on two counts: (i) The 1.1% natural abundance of the ^{13}C nuclei is too low to account for the ratio I_{sat}/I_c of the intensity of the satellites to that of the central resonances, which is ~ 0.04 and increases to ~ 0.09 upon annealing (see below). (ii) Hyperfine coupling with ^{13}C should lead to a constant value of I_{sat}/I_c , i.e., an overall line shape which should not vary from sample to sample. Figures 1(a) and 1(b) clearly show that the resolution of the satellites does vary considerably. Indeed, in some films deposited from methanol, ethanol, or other oxygen-containing precursors, their intensity is negligible.^{4,7} This observation is discussed below. We also note that the splitting of these satellites from the main Lorentzians at $g = 2.0028 \pm 0.0005$ is $\Delta H \approx \pm 6$ G in the samples studied by Redwing, Root, and Banholzer⁶ but ± 7.2 G in the samples studied in this work.

Previous ^1H NMR measurements have indicated that most of the hydrogen in thin diamond films resides on the crystallite surfaces, and most of it is removed after ~ 2 -hr annealing at $\sim 850^\circ\text{C}$.^{6,10-13} Sample *B* was therefore annealed in 1-h steps, and its ESR was measured after each step. Yet in spite of annealing in an Ar flow at 740, 765, 790, 830, 867, 905, 935, 965, 1013, 1057, and 1085 $^\circ\text{C}$, then crushing it to a powder and annealing it in an evacuated quartz tube at 828, 865, and 970 $^\circ\text{C}$, and then crush-

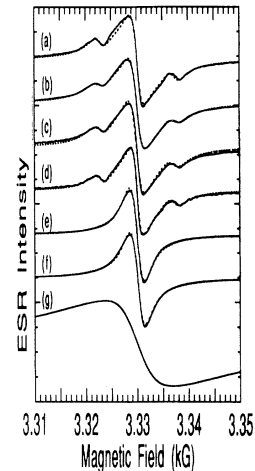


FIG. 1. X-band ESR spectra (solid lines) of thin diamond films. The dotted lines are the sum of four [spectra (a)–(d)] or two [spectra (e) and (f)] Lorentzians, of *g* values, amplitudes, and linewidths listed in Table I. (a) Sample *A*, as deposited for 30 h from a mixture of 99.5% H_2 and 0.5% CH_4 (see text for details). (b) Sample *B*, as deposited under the same conditions, but for 146 h. Note that the satellites are weaker relative to the central resonances than in (a). (c) Sample *B* following 1-h annealing steps (see text) at $T \leq 1112^\circ\text{C}$. (d) Same sample, after annealing by an oxyacetylene torch for 20 min at $\sim 1500^\circ\text{C}$ in an Ar flow. (e) Sample *C*, as deposited from a mixture of 99.5% D_2 and 0.5% CD_4 . Note the absence of the satellites from this spectrum. (f) Sample *D*, as deposited from a mixture of 99.5% D_2 and 0.5% CH_4 . Note that the satellites are absent from this ESR as well. (g) Sample *E*, as deposited from a mixture of 99.5% H_2 and 0.5% $^{13}\text{CH}_4$. Note the inhomogeneous broadening due to the hyperfine coupling of the dangling bonds with the ^{13}C nuclei.

ing the powder further and annealing it in an Ar flow at 805, 875, 965, 1015, and 1112 $^\circ\text{C}$, the ESR line shape and spin density did not change [Fig. 1(c)]. Finally, the sample was heated for 20 min in an Ar flow by an oxyacetylene torch at $\sim 1500^\circ\text{C}$, as measured by an optical pyrometer; the resulting ESR is shown in Fig. 1(d). Interestingly enough, while the overall spin density decreased by a factor of ~ 4.5 , the relative intensity of the satellites slightly *increased* with respect to the main lines (Table I).

Figure 1(e) shows the ESR spectrum of sample *C* simi-

TABLE I. The spin densities N_s of the samples whose ESR spectra are shown in Fig. 1, the derivative peak-to-peak linewidth and fractional integrated intensity of the central narrow (ΔH_{ppn} and I_n , respectively) and broad (ΔH_{ppb} and I_b , respectively) Lorentzians, and those of the satellites (ΔH_{ppsat} and I_{sat} , respectively). In all cases, the *g* values of the central Lorentzians are 2.0028 ± 0.0005 , and the satellites are split from them by $\Delta H = 7.2 \pm 0.2$ G.

Sample Spectrum	<i>A</i> 1(a)	<i>B</i> 1(b)	<i>B</i> 1(c)	<i>B</i> 1(d)	<i>C</i> 1(e)	<i>D</i> 1(f)	<i>E</i> 1(g)
N_s (gm^{-1})	3.1×10^{16}	2.7×10^{17}	2.7×10^{17}	6.2×10^{16}	1.1×10^{18}	1.4×10^{18}	3.6×10^{17}
N_s (ppm)	0.6	5.4	5.4	1.2	22	28	7.8
ΔH_{ppn} (G)	2.4	2.6	2.6	1.9	2.8	2.9	
I_n (%)	12	13	15	10	44	35	
ΔH_{ppb}	7.5	7.8	7.5	5.8	8.7	10.1	
I_b (%)	83	83	78	81	56	65	
ΔH_{ppsat}	2.4	2.9	3.0	2.7			
I_{sat} (%)	5	4	7	9			

larly deposited from a mixture of 99.5% D₂ and 0.5% CD₄. As clearly seen from the figure and Table I, the satellites are completely absent from this sample. Also striking is the increased intensity of the central narrow Lorentzian relative to the broad component. It is suspected, however, that this is due to the contribution of unresolved ²D-hyperfine-split dangling bonds. Figure 1(f) shows the ESR of sample *D* deposited from 99.5% D₂ and 0.5% CH₄. As in Fig. 1(e), the satellites are absent from this film as well, and the central narrow Lorentzian is relatively much more intense than in Figs. 1(a)–1(d). Finally, Fig. 1(g) shows the ESR of the fully ¹³C-enriched film (sample *E*). Its inhomogeneously broadened structureless line shape ($\Delta H_{pp} \approx 13$ G) is clearly due to the hyperfine coupling of the dangling bonds to the central and neighboring ¹³C nuclei.

¹³C NMR relaxation measurements on the fully ¹³C-enriched sample *E* and naturally abundant (1.1%) ¹³C sample *F*, each deposited under conditions similar to those of sample *B*, yielded an exponential recovery of the free-induction decay in all cases. Their paramagnetic spin densities and ¹³C *T*₁'s are summarized in Table II. Since spin diffusion¹⁶ to these defects is believed to be the dominant ¹³C relaxation mechanism, the defect distribution should strongly affect *T*₁. The results clearly indicate that the dangling-bond distribution is probably homogeneous, rather than confined to the crystallite surfaces: (a) The ¹³C spin diffusion constant in diamond can be estimated to be $D \approx 0.15\gamma^2\hbar d$,¹⁷ where γ is the ¹³C gyromagnetic ratio and *d* is the mean ¹³C–¹³C distance. This yields $D_E \approx 4 \times 10^{-13}$ and $D_F \approx 0.85 \times 10^{-13}$ cm²/s for samples *E* and *F*, respectively. Therefore, during time *T*₁ the ¹³C magnetization is transported over a distance of $\sim \sqrt{6DT_1}$, or ~ 0.04 μm in both samples *E* and *F* (Table II). However, this value is much smaller than the average crystallite size, especially in sample *F* (Table II). (b) The distribution of crystallite sizes is apparently very broad, from a fraction of a micrometer near the substrate to several micrometers near the top surface.^{10,11,14,15} Therefore, confinement of the dangling bonds to the crystallite surfaces should result in a striking deviation from an exponential relaxation, in contrast to the observed simple exponential recovery of the ¹³C magnetization.¹⁴ (c) An additional argument related to the ratio of *T*_{1E}/*T*_{1F}, which also strongly indicates that the distribution of the paramagnetic center is homogeneous rather than confined to the crystallite surfaces, is described elsewhere.¹⁴

The foregoing ESR results clearly show that the satellites are due to carbon dangling bonds hyperfine coupled to adjacent protons. The hyperfine coupling constant of these H–dangling-bond complexes is equal to the field splitting between the two satellites, i.e., about 14.5 G (13.5×10^{-4} cm⁻¹). Their intensity indicates that their

density is about 0.03–0.2 ppm (Table I), i.e., they are a minute fraction of the total H content, which is several thousand ppm (Table II) as determined by ¹H NMR. Indeed, they do not even contribute to the NMR, as the resonance frequency and spin-lattice relaxation rate of nuclei adjacent to paramagnetic defects generally render them invisible by NMR.

The stability of the satellites upon annealing at $T \leq 1100$ °C for extended periods strongly suggests that the H–dangling-bond complexes are not on any crystallite surface. However, the reduction of the satellites and the main line by a factor of ~ 4.5 after ~ 20 -min annealing at ~ 1500 °C is consistent with the evolution of most of the hydrogen from these centers. We therefore consider two types of bulk hydrogen–dangling-bond centers: A center on an internal surface, and a center trapped in the tetrahedral diamond network.

As mentioned above, SEM images showed that the average crystallite is several micrometers across at the top surface of the films. Yet if the hydrogen is essentially confined to the crystallite surfaces, then the ¹H NMR spin count indicates that the average crystallite is less than 0.5 μm across (see Table II). As mentioned above, this discrepancy may be resolved by previous observations which showed that the crystallite size rapidly increases during film growth.^{10,11,15} This apparent discrepancy therefore does not allude to the existence of internal surfaces within the observed crystallites. However, such internal surfaces and/or microvoids are to be expected within the kinetic model described by Anthony.¹⁸ In this model, the hydrogenated surface is constantly etched and repassivated by H atoms, but occasionally a methyl radical¹⁹ attaches to an exposed carbon dangling bond, providing the fundamental diamond network growth step. Such dynamical processes may yield considerable internal defect structures and (micro)surfaces. However, if a significant fraction of the hydrogen that is observed by NMR (i.e., not neighboring a dangling bond) resides on these surfaces, it too is released within a few hours at ~ 850 °C. Yet the observed spectra clearly suggest the presence of an H atom in a center that is unaffected by annealing at $T \leq 1100$ °C. The scenario of relatively large hydrogen-decorated internal surfaces is thus apparently unrelated to the dangling-bond–H center observed by the ESR. We therefore turn to the model of a dangling-bond–H center which is embedded in the bulk of the tetrahedral network.

In the simplest approach, substitution of a C by a H atom should result in a H atom terminating one dangling bond and an interacting system of the three other dangling bonds. The ground state of this system should probably be an unpaired *sp*³ electron slightly overlapping the reconstructed paired wave function of the other two, as carbon bonds pair on diamond surfaces.^{18,20,21} Howev-

TABLE II. NMR and ESR parameters of sample *E* (fully ¹³C-enriched film) and sample *F* (natural 1.1% abundant ¹³C): Dangling-bond spin density *N*_s, ¹³C spin-lattice relaxation time *T*₁, proton spin density of H content *N*_H, and estimated average diamond crystallite size *a* (Ref. 14).

Sample	<i>N</i> _s (gm ⁻¹)	<i>N</i> _s (ppm)	<i>T</i> ₁ (s)	<i>N</i> _H (gm ⁻¹)	<i>N</i> _H (at. %)	<i>a</i> (μm)
<i>E</i>	3.6×10^{17}	7.8	6±1	2.6×10^{20}	0.55	0.12
<i>F</i>	4.4×10^{17}	8.8	27±3	7.3×10^{19}	0.15	0.43

er, this model should be verified by a calculation of the defect wave function which would yield a ^1H hyperfine splitting in agreement with the observed value. Given the strong C-H bond and the surrounding tetrahedral diamond network, the stability of these centers at $T \leq 1100^\circ\text{C}$ is not necessarily improbable, but also needs to be substantiated by simulations of H dynamics in such centers and in the diamond lattice. At the same time, the reduction in their intensity after 20 min at 1500°C (Table I) is consistent with evolution of hydrogen from these centers at such high temperatures.

While a bulk dangling-bond-H center is suggested to be responsible for the satellites of the ESR, the nature of the main lines is not clear. The dynamics of the main lines appear to be similar to that of the satellites [Figs. 1(b)–1(d) and Table I]. In considering the main lines in terms of a bulk center, however, one would expect a C vacancy to reconstruct to two spinless paired bonds.¹⁸ Some interesting speculations may include a substitutional oxygen, W, Ta, or other metal atom present in the deposition chamber. Yet these should be even more stable than the dangling-bond-H center, in contrast to the slight but unambiguous weakening of the central lines relative to the satellites after annealing at $\sim 1500^\circ\text{C}$. Thus, in spite of dynamics similar to that of the satellites, we consider dangling bonds on internal defect surfaces. Although these would be hyperfine coupled to adjacent ^1H , the dangling-bond- ^1H distance might be sufficiently larger than that in the bulk center to yield a hyperfine coupling that would be unresolved from an $\sim 7\text{-G}$ -wide envelope. The narrower line might then indeed result from an exchange-narrowed odd-numbered cluster of dangling bonds, as suggested by Redwing, Root, and Banholzer,⁶ on an internal defect surface.

The absence of the ^1H -coupled dangling bonds from some films prepared by CVD from oxygen-containing precursors^{4,7} suggests that these precursors, under appropriate conditions, prevent the formation of such H-dangling-bond centers. It also indicates that the H-dangling-bond center probably does not include an

oxygen atom. The role of the oxygen-containing precursors in preventing the appearance of the satellites of the ESR is not clear, however. In any case, though, the reduced content of these centers in films deposited from such precursors may be significant for the optoelectronic properties of the films, as such centers should efficiently trap photogenerated or injected carrier.

Figure 1(e) showed that the ^1H -hyperfine coupled dangling bonds are absent from films deposited from 99.5% D_2 and 0.5% CH_4 . This suggests that the probability of incorporation of H or D is unrelated to its source. It also then suggests that most of the H or D atoms that are found on the surfaces of the diamond crystallites are due to the H_2 or D_2 gas, rather than to the hydrogen attached to the carbon-containing precursor.

In summary, the X-band ESR of thin diamond films deposited from a mixture of 99.5% H_2 and 0.5% CH_4 invariably exhibits Lorentzian satellites at $\Delta H \approx 7.2 \pm 0.2\text{ G}$ from the main line at $g \approx 2.0028 \pm 0.0005$, which is the sum of narrow ($\Delta H_{ppn} \approx 2.4 \pm 0.2\text{ G}$) and broad ($\Delta H_{ppb} \approx 7.6\text{ G}$) Lorentzians. As the ESR of films deposited from a mixture of 99.5% D_2 and 0.5% CD_4 or 0.5% CH_4 does not exhibit the satellites, they are assigned to dangling-bond-H complexes. The main lines and the satellites are unaffected by annealing at $T \leq 1100^\circ\text{C}$, but are reduced after ~ 20 min at $\sim 1500^\circ\text{C}$. The complexes are thus discussed in relation to newly identified dangling-bond-H centers on internal surfaces, or embedded in the bulk of the diamond crystallites. The latter scenario appears to be more plausible if confirmed by a calculation of the defect wave function which would yield a ^1H hyperfine splitting in agreement with the observed value of $\sim 13.5 \times 10^{-4}\text{ cm}^{-1}$.

We thank Dr. K. K. Gleason, Dr. S. Mitra, Dr. R. Shinar, Dr. S. T. Pantelides, Dr. W. Trahanovsky, Dr. K. M. Ho, and Dr. R. Biswas for valuable discussions. Ames Laboratory is operated by Iowa State University for the U.S. Department of Energy under Contract No. W-7405-Eng-82. This work was supported by the Director for Energy Research, Office of Basic Energy Sciences.

¹*Diamond, Silicon Carbide, and Related Wide Bandgap Semiconductors*, edited by J. T. Glass, R. Messier, and N. Fujimori, MRS Symposia Proceedings No. 162 (Materials Research Society, Pittsburgh, 1990).

²*Wide Band Gap Semiconductors*, edited by T. D. Moustakas, J. I. Pankove, and Y. Hamakawa, MRS Symposia Proceedings No. 242 (Materials Research Society, Pittsburgh, 1992).

³A. T. Collins, in *Diamond, Silicon Carbide, and Related Wide Bandgap Semiconductors* (Ref. 1), p. 3.

⁴I. Watanabe and K. Sugata, *Jpn. J. Appl. Phys.* **27**, 1808 (1988).

⁵M. Hoinkis, E. R. Weber, M. I. Landstrass, M. A. Plano, S. Han, and D. R. Kania, *Appl. Phys. Lett.* **59**, 1870 (1991).

⁶J. M. Redwing, T. W. Root, and W. F. Banholzer (unpublished).

⁷H. Jia, J. Shinar, S. Mitra, and K. K. Gleason (unpublished).

⁸J. H. N. Loubser and J. A. van Wyk, *Rep. Prog. Phys.* **41**, 1201 (1978).

⁹H. B. Dyer and L. du Preez, *J. Chem. Phys.* **42**, 1898 (1965); H. B. Dyer, F. A. Raal, L. du Preez, and J. H. N. Loubser, *Philos. Mag.* **11**, 763 (1965).

¹⁰K. M. McNamara, D. H. Levy, K. K. Gleason, and C. J. Ro-

binson, *Appl. Phys. Lett.* **60**, 580 (1992).

¹¹K. M. McNamara, K. K. Gleason, and C. J. Robinson, *J. Vac. Sci. Technol. A* **10**, 3143 (1992).

¹²D. H. Levy and K. K. Gleason, *J. Phys. Chem.* **96**, 8125 (1992).

¹³S. Mitra and K. K. Gleason, *Diamond Relat. Mater.* **2**, 126 (1993).

¹⁴D. P. Lang, M. Pruski, H. Jia, and J. Shinar (unpublished).

¹⁵Ch. Wild, N. Herres, and P. Koidl, *J. Appl. Phys.* **68**, 973 (1990).

¹⁶A. Abragam, *Principles of Nuclear Magnetism* (Oxford University Press, Oxford, 1961), Chap. 9.

¹⁷M. Goldman, *Phys. Rev.* **138**, A1675 (1965).

¹⁸T. R. Anthony, in *Diamond, Silicon Carbide, and Related Wide Bandgap Semiconductors* (Ref. 1), p. 61.

¹⁹M. R. Pederson, K. A. Jackson, and W. E. Pickett, in *Diamond, Silicon Carbide, and Related Wide Bandgap Semiconductors* (Ref. 1), p. 91.

²⁰S. T. Pantelides (private communication).

²¹W. Trahanovsky (private communication).